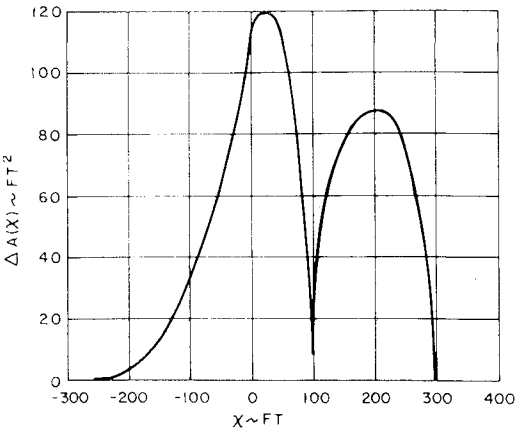

Fig. 2 Area distribution required of addition scheme.

$$\tilde{m}(x) = \rho_\infty U_\infty \Delta A(x) \tag{4}$$

Since the maximum area change required is about 120 ft², it is found that a maximum mass flow of approximately 2500 lb/sec is required. This estimate is conservative since the actual density contributions up to the body station where the maximum area change occurs will increase the result. This mass flow rate is about the total capability of the SST engines.[7] If the additional weight necessary to cycle this mass flow is estimated as that of the engines plus the additional fuel to run a second set of engines, the total weight penalty without considering the additional lift required is prohibitive even for a perfect system. In addition, if only 10 lb/sec were not reclaimed, it would result in a loss of over 100,000lb of material during the course of a three hour flight. The question of whether heat addition is possibly more effective can be answered by applying the analysis embodied in Eqs. (3) in an approximate manner. A "most favorable" estimate will be obtained by neglecting the pressure interaction since there will then be no induced counter force to oppose the area growth. The result of this procedure is

$$\int_{x_0}^{x} \dot{q}(t)dt = \frac{\gamma}{\gamma - 1}\left[P_\infty U_\infty (\Delta A(x) - A_0)\right] \tag{5}$$

where X_0 is the station at which $\Delta A(X_0) = A_0$.

Since the continuity and momentum equations result in the fact that $\rho A = \text{const}$, reasonable upper limits of the area ratio can be deduced by imposing limits on the temperatures to be reached.† At an area ratio of $\Delta A_{max}/A_0 = 9$, one obtains a power level of $\frac{1}{3}$ million horsepower which is approximately 70% of the engine capability. The weight penalties are, therefore, essentially the same as in the mass addition case. If one attempts to produce "lower bound" shapes using these schemes the weight penalties increase. The energy required to obtain the maximum area change, ΔA_{max}, falls to zero as the reference streamtube's initial area approaches ΔA_{max}. In this case, there will be no area variation of the reference streamtube and consequently the required phantom boundary shape ($\alpha X^{5/2}$) will not be obtained. If large initial streamtube areas are to be considered, the final area change must be allowed to increase such that the proper distribution is attained. This will involve larger volumes of air and, hence, even more power than estimated previously.

In summary, simple techniques by which the effects of mass and energy addition upon the area distribution may be assessed have been presented. Also presented were the results of some sample calculations which indicate that the mass and energy addition schemes are probably not competitive with configurational changes as sonic boom minimization techniques.‡

† It is postulated that the transition from supersonic to subsonic flow is indicative of strong shock generation and should be avoided.

References

[1] Cahn, M. S. and Andrew, G. M., "Electroaerodynamics in Supersonic Flow," AIAA Paper 68-24, New York, Jan. 1968.

[2] Cheng, S. I. and Goldburg, A., "An Analysis of the Possibility of Reduction of Sonic Boom by Electro-Aerodynamic Devices," AIAA Paper 69-38, New York, Jan. 1969.

[3] McLean, F. E., "Configuration Design for Specified Pressure Signature Characteristics," SP-180, 1968, NASA.

[4] McLean, F. E. and Carlson, H. W., "Sonic Boom Characteristics of Proposed Supersonic and Hypersonic Airplanes," TND-3587, 1966, NASA.

[5] Liepmann, H. W. and Roshko, A., "Elements of Gasdynamics," Wiley, New York, 1958, pp. 223–237.

[6] Walkden, F., "The Shock Pattern of a Wing-Body Combination Far from the Flight Path," *Aeronautics Quarterly*, Vol. 9, Pt. 2, May 1958, pp. 164–194.

[7] *Jane's All the World's Aircraft*, 1968–1969 edition, McGraw-Hill, New York, pp. 237, 649.

[8] Miller, D. S. and Carlson, H. W., "A Study of the Application of Heat or Force Fields to the Sonic Boom Minimization Problem," TN D-5582, Dec. 1969, NASA.

‡ Since submittal of this Note, Miller and Carlson[8] have published a similar analysis. Their findings are also similar to to those presented previously.

Subsonic Lift Interference in a Wind Tunnel with Perforated Walls

CHING-FANG LO*
ARO Inc., Arnold Air Force Station, Tenn.
AND
ROBERT H. OLIVER†
University of Tennessee Space Institute, Tullahoma, Tenn.

Introduction

THE development of large, high subsonic speed aircraft requires rather accurate wind-tunnel data for aerodynamic design. Testing for such aircraft has normally been performed in transonic wind tunnels that have ventilated test sections such as the transonic wind tunnels at Arnold Engineering Development Center. Historically, the perforated walls were developed to minimize blockage interference at low supersonic Mach numbers by using a nonlifting, cone-cylinder model.[1] As a result, corrections to the data for a lifting-body model are necessary to obtain accurate data. This fact was pointed out in a recent study of wind-tunnel data correlation[2] where it was concluded that wind-tunnel wall effects must be taken into account to improve the quality of test data.

It is indicated in Ref. 3 that there is no available analytical solution for the boundary interference in a wind tunnel with perforated walls. The only existing solution has been obtained by an electrical analog measurement[4] for the case of a square tunnel with four walls perforated.

The purpose of this Note is to present an analytical solution of the boundary interference for wind tunnels with perforated walls. The method used in the calculation is the

Received December 31, 1969. The research reported herein was sponsored by the Arnold Engineering Development Center, Air Force Systems Command, under Contract No. F40(600)-69-C-0001 with ARO Inc. Further reproduction is authorized to satisfy needs of the U.S. Government.

* Research Engineer, Propulsion Wind Tunnel Facility; also Assistant Professor, Aerospace Engineering Department (part time), University of Tennessee Space Institute. Member AIAA.

† Research Assistant, Department of Aerospace Engineering. Member AIAA.

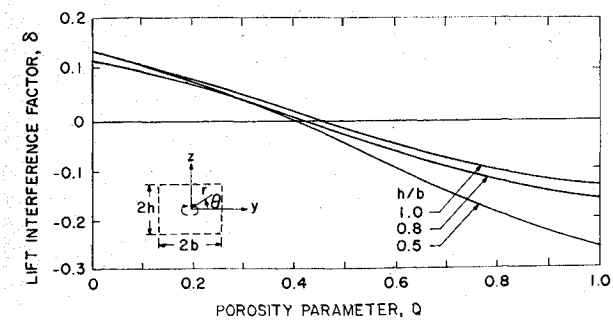

Fig. 1 Lift interference factor at the model position for rectangular tunnels with all walls perforated, $Q_v = Q_h = Q$.

point-matching method in conjunction with Fourier transforms, which has been used previously in the slotted-wall tunnel.[5] The material contained in this Note concerns the results for lift interference only. The solid and wake blockage interferences may be found in Ref. 6.

General Analysis

The field equation of an inviscid, irrotational fluid for subsonic flow in terms of the perturbation velocity potential φ in cylindrical coordinate is

$$[(\beta^2(\partial^2/\partial x^2) + (\partial^2/\partial r^2) + (\partial/r\partial r) + (1/r^2)\partial^2/(\partial\theta^2)]\varphi = 0 \quad (1)$$

The boundary condition for a perforated wall is derived[7] in an average sense as

$$(\partial\varphi/\partial x) + (1/R)\partial\varphi/\partial n = 0 \quad (2)$$

where R is the porosity parameter which is an empirical constant; it was measured in Ref. 1 for a sample wall. In this Note, a related porosity parameter is introduced as $Q = (1 + \beta/R)^{-1}$ where the value of $Q = 0$ corresponds to a closed wall and $Q = 1$ to an open wall.

The linearity of the field equation and its boundary condition permits the perturbation potential to be separated into two parts as

$$\varphi = \varphi_m + \varphi_i \quad (3)$$

where φ_m = the disturbance potential caused by a model and φ_i = the interference potential induced by the tunnel boundary. A horseshoe vortex is used as the mathematical model for the disturbance potential in the calculation of the lift interference. A doublet and a source can be used in the calculation of solid and wake blockage interference, respectively.[6] The interference potential φ_i is obtained by Fourier transform in conjunction with point-matching method.[5]

For rectangular test sections where the vertical walls and horizontal walls having different porosities, the transformed

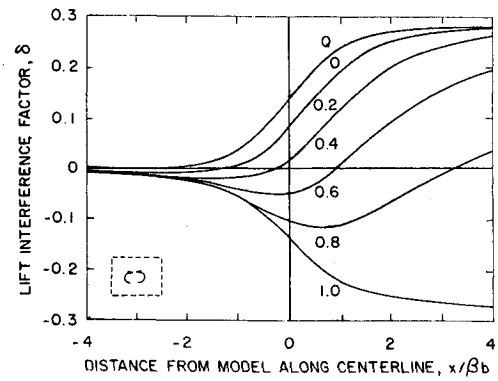

Fig. 2 Distribution of the lift interference factor along the centerline of a square wind tunnel with all walls perforated, $Q_v = Q_h = Q$.

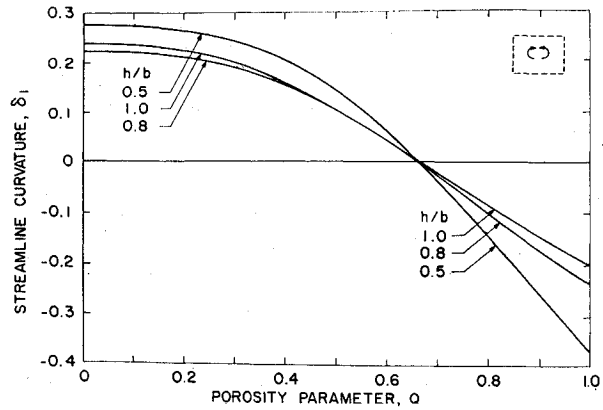

Fig. 3 Streamline curvature at the model position for rectangular wind Tunnels with all walls perforated, $Q_v = Q_h = Q$.

solution $\bar{\varphi}_i$ of the interference potential may be written as a series solution with undetermined constants in the form

$$\bar{\varphi}_i = \sum_{m=0}^{\infty} [C_{1m}\cos m\theta + C_{2m}\sin m\theta] I_m\left(\frac{qr}{b}\right) \quad (4)$$

where

$$\bar{\varphi}_i = (2\pi)^{-1/2}\int_{-\infty}^{\infty} \varphi_i e^{iqx/\beta b}\, dx, \quad (5)$$

I_m = modified Bessel function

The undetermined constants C_{1m}, C_{2m} are determined by using the transformed boundary conditions

$$-iq\bar{\varphi}_i \pm (b\beta/R_v)\partial\bar{\varphi}_i/\partial y = -[-iq\bar{\varphi}_m \pm (b\beta/R_v)\partial\bar{\varphi}_m/\partial y] \text{ at } y = \pm b \quad (6)$$

$$-iq\bar{\varphi}_i \pm (b\beta/R_h)\partial\bar{\varphi}_i/\partial z = -[-iq\bar{\varphi}_m \pm (b\beta/R_h)\partial\bar{\varphi}_m/\partial z] \text{ at } z = \pm h \quad (7)$$

where

$$\bar{\varphi}_m = (2\pi)^{-1/2}\int_{-\infty}^{\infty} \varphi_m e^{iqx/\beta b}\, dx \quad (8)$$

The series solution Eq. (4) is truncated at a finite term M. A set of simultaneous linear algebraic equations can be obtained by substituting Eq. (4) into Eqs. (6) and (7) and selecting $2M$ discrete points uniformly distributed along the boundary. Improved accuracy is achieved, however, by selecting more than $2M$ points along the boundary and calculating C_{1m}, C_{2m} by satisfying the boundary condition in the least-squares sense. Once the transformed potential $\bar{\varphi}_i$ is obtained, then the interference potential in the physical plane is determined by the inversion formula.

Lift Interference

The lift interference is calculated using a horseshoe vortex to represent the wing model. The potential of the wing with

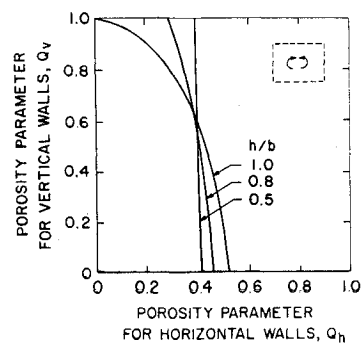

Fig. 4 Zero lift interference curves for rectangular perforated tunnels.

circulation Γ at the origin is given by

$$\varphi_m = \frac{\Gamma s}{2\pi}\frac{\sin\theta}{r} + \frac{\Gamma s}{2\pi}\frac{\sin\theta}{r}\frac{x}{(x^2+\beta^2r^2)^{1/2}} = \varphi_{m_1}(r,\theta) + \varphi_{m_2}(x,r,\theta) \quad (9)$$

Since the disturbance potential consists of two terms, one independent of x and the other dependent of x, the interference potential may be split into two parts as

$$\varphi_i = \varphi_{i_1}(r,\theta) + \varphi_{i_2}(x,r,\theta) \quad (10)$$

The potential φ_{i_1}, induced by φ_{m_1}, is found as

$$\varphi_{i_1} = \frac{\Gamma s}{2\pi b}\sum_{m=1,3,5}^{\infty} D_m r^m \sin m\theta \quad (11)$$

The transformed potential $\tilde{\varphi}_{i_2}$, due to φ_{m_2}, is reduced from Eq. (4) to

$$\tilde{\varphi}_{i_2} = \sum_{m=1,3,5}^{\infty}(G_m + iE_m)\sin m\theta I_m\left(\frac{qr}{b}\right) \quad (12)$$

The coefficients D_m, G_m, and E_m are determined from matching the boundary conditions at discrete points by the point-matching method.

The interference potential is obtained from Eqs. (11) and (12)

$$\varphi_i(x,r,\theta) = \frac{\Gamma s}{2\pi b}\left\{\sum_{m=1,3,5}^{\infty} D_m r^m \sin m\theta + \frac{2}{\pi}\int_0^{\infty}\sum_{m=1,3,5}^{\infty}\sin(m\theta)I_m\left(\frac{qr}{b}\right)\left[G_m\cos\left(\frac{qx}{\beta b}\right) + E_m\sin\left(\frac{qx}{\beta b}\right)\right]dq\right\} \quad (13)$$

The lift interference factor δ and the streamline curvature δ_1 are defined as

$$\delta = \frac{C}{SC_L}\frac{1}{U}\frac{\partial\varphi_i}{\partial z} \text{ and } \delta_1 = \frac{2\beta h}{S}\frac{C}{C_L}\frac{1}{U}\left(\frac{\partial^2\varphi_i}{\partial x\,\partial z}\right)_{r=0}$$

respectively.

The lift interference factor and its distribution along the centerline are shown in Figs. 1 and 2 for test sections of various height-to-width ratios and different porosities. Figure 3 shows the streamline curvature at the model position.

All numerical results presented herein were determined by using ten terms of the infinite series and twenty points along one quadrant of the boundary because of the symmetrical property of this problem. In order to examine the accuracy of the present method, the case of closed vertical walls and perforated horizontal walls has been calculated and compared with the results obtained in a closed form by another method in Ref. 8. The comparison indicates excellent agreement for the case of a square or nearly square tunnel and satisfactory agreement for the case of test sections having height-to-width ratios around 0.5. Similar results have been noted for a slotted wall tunnel as previously reported in Ref. 5.

It is interesting to note that zero interference can be obtained by the proper combination of porosity in the horizontal and vertical walls. The proper combination of porosity required for zero lift interference is shown in Fig. 4 and indicates the lift interference is insensitive to the porosity of the vertical walls for height-to-width ratios less than 0.8, as is also the case for the slotted wall tunnel.[5]

References

[1] Pindzola, M. and Chew, W. L., "A Summary of Perforated Wall Wind Tunnel Studies at the Arnold Engineering Development Center," TR-60-9, Aug. 1960, Arnold Engineering Development Center.

[2] Treon, S. L. et al., "Data Correlation from Investigation of a High-Subsonic Speed Transport Aircraft Model in Three Major Transonic Wind Tunnels," AIAA Paper 69-794, Los Angeles, Calif., 1969.

[3] Garner, H. C. et al., "Subsonic Wind Tunnel Wall Corrections," AGARDograph 109, Oct. 1966.

[4] Rushton, K. R. and Laing, L. M., "A General Method of Studying Steady Lift Interference in Slotted and Perforated Tunnels," R and M 3567, 1968, Aeronautical Research Council.

[5] Lo, C. F. and Binion, T. W., Jr., "A V/STOL Wind Tunnel Wall Interference Study," AIAA Paper 69-171, New York, 1969; also *Journal of Aircraft*, Vol. 7, No. 1, Jan.-Feb. 1970, pp. 51–57.

[6] Lo, C. F. and Oliver, R. H. "Boundary Interference in a Rectangular Wind Tunnel Wire Perforated Walls,"TR-70-67, April 1970, Arnold Engineering Development Center.

[7] Goodman, T. R., "The Porous Wall Wind Tunnel, Part II. Interference Effect on a Cylindrical Body in a Two-Dimensional Tunnel at Subsonic Speed," Rept. AD-594-A-3, 1950, Cornell Aeronautical Lab. Inc.

[8] Oliver, R. H., "Determination of Blockage and Lift Interference for Rectangular Wind Tunnels with Perforated Walls," MS thesis, Aug. 1969, University of Tennessee, Knoxville, Tenn.

Simplified Analysis of a Trifragment Rotor Disk Interaction with a Containment Ring

R. Bruce McCallum*

Massachusetts Institute of Technology, Cambridge, Mass.

Introduction

RECENT spin-pit tests have been performed at the Naval Air Propulsion Test Center, Philadelphia, Pa. on 15-in.-i.d. steel rings of various thicknesses using comparatively nondeforming steel fragments (as illustrated in Fig. 2) to evaluate the possibility of using an inexpensive standard fragment generator in future parametric studies. The purpose of these parametric studies would be to test the merits of various materials to be used for jet engine burst rotor containment devices. In those tests where containment-ring failure occurred, high-speed photographs show a "shattering" effect, where the ring appears to separate in one or more locations with little noticeable deformation, within 400 μsec after collision. Since other tests, using bladed rotor segments as fragments, show considerable ring deformation before ring failure occurs, the use of nondeforming fragments has been considered by some as an unsatisfactory substitute for the more expensive bladed-rotor fragments.

In the present Note, the results of an analysis (using a computer program written at Massachusetts Institute of

Received January 29, 1970. This research is supported by Grant No. NGR 22-009-339 from the Aerospace Safety Research and Data Institute, Lewis Research Center, NASA, Cleveland, Ohio. The author is indebted to A. A. Martino and G. J. Mangano of Naval Air Propulsion Test Center., Philadelphia for their experimental data, and he gratefully acknowledges the comments and advice given to him by E. A. Witmer and J. W. Leech of Aeroelastic and Structures Research Laboratory, Massachusetts Institute of Technology. The computations were carried out at the Massachusetts Institute of Technology Information Processing Center.

* Senior Research Engineer, Aeroelastic and Structures Research Laboratory.